5.1 Introduction

Dopamine (DA) is a neurotransmitter that plays a crucial role in the central nervous, cardiovascular, renal system and endocrine systems. In the case of Parkinson's disease, the concentration of DA in the extracellular fluid is an important parameter to be used in diagnostics [1]. Due to its use in health monitoring and diagnostics, the detection of physiologically relevant chemicals using electrocatalysts is a highly investigated topic. Numerous biomolecules have been selected for non-enzymatic sensing employing electrocatalysts, including glucose, dopamine, uric acid, ascorbic acid, lactic acid, and catechol [2–4]. Several major disorders, including schizophrenia, Huntington's, attention-deficit hyper activity disorder (ADHD), Parkinson's, and Alzheimer's are indicated by abnormal levels of DA in bodily fluids [5]. Due to their accuracy, affordability, ease of use, and rapid response to the determination of DA, electrochemical sensor systems appear to be an adequate way to detect DA when compared to the currently used analytical methods including surface enhanced Raman scattering (SERS), chemiluminescence, fluorescence, chromatography, and other similar techniques [6–9]. The electrochemical approach gains popularity due to its simplicity, affordability, specificity, and quick analysis [10,11]. Because of their similar oxidation potentials, ascorbic acid (AA) and uric acid (UA) can confound DA detection at conventional electrodes, leading to inadequate findings [12,13].

A highly sensitive and selective sensor platform is required to monitor disease progression effectively and manage medical care by accurately detecting dopamine levels. The electrode surface fouling is a prevalent and significant concern in numerous electrochemical investigations. This impaired the properties of electrochemical sensors like reproducibility, sensitivity, detection limit, and overall performance. Many antifouling approaches involve

employing an electrode that has been modified to exhibit higher resistance to fouling compared to an unmodified electrode [14–16]. To overcome the electrode fouling problem for the detection of dopamine, several catalysts have been developed. In particular, carbon-based compounds such as multi-walled carbon nanotubes (MWCNTs), and carbon nanotubes (CNTs) are promising materials due to their high conductivity, low resistance to chemical reactions, high specific area, low surface fouling, and capacity to speed up electrochemical reactions [17–19]. Electrode modification is widely employed using bimetallic nanoparticles, including combinations of nickel, palladium, platinum, iron, and gold-based nanoparticles, due to their intriguing physical, chemical, and distinctive electrocatalytic properties.

Over the past few decades, a wide range of bimetallic nanoparticles has undergone extensive research for a number of crucial catalytic processes, the extremely distinctive chemical and physical characteristics and the potential for specialized catalytic activities, metal NPs are of utmost significance [20]. Due to their numerous oxidation states for electron-transfer processes, transition metal nanoparticles have recently attracted a growing deal of interest. Nickel nanoparticles (Ni NPs), in particular, have been employed widely in electrode modification due to their intrinsic electrocatalytic ability for oxidation reactions [21]. Palladium-nickel (Pd-Ni) is a combination of metals that has been studied extensively because it is more effective than Pd monometallic catalysts in many crucial industrial processes [22,23]. The alteration of the working electrode with unique high-performance nanomaterials has evolved into the direction of our efforts as we anticipate the development of ultrasensitive electrochemical sensors. In this study, a new electrochemical sensor for DA detection was created using Ni-Pd nanoparticle decorated on an f-MWCNT-modified carbon paste electrode.

Ferrocene monocarboxylic acid was used as redox mediators during the modification of electrodes.

5.2 Experimental

5.2.1 Materials

Sodium dihydrogen phosphate (NaH_2PO_4), disodium hydrogen phosphate (Na_2HPO_4), and potassium tetrachloropalladate (K_2PdCl_4) were purchased from Merck while dopamine (DA), MWCNT, and nickel chloride were procured from Sigma Aldrich. Oleylamine was purchased from SRL India. The dopamine injection sample was purchased from Sunvet Pharma Pvt. Ltd. All chemicals and reagents were of the finest purity and used exactly as provided.

5.2.2 Synthesis of nickel nanoparticles

Aqueous solution of 20 mM $NiCl_2.6H_2O$ was prepared and add 50 µl of $NaBH_4$ (0.2 M), 50 µl Oleylamine (methanolic solution) in a round bottom flask, mix the solution vigorously, and add 40-60 µl of 0.5 M NaOH. Stirred the mixture on a hotplate stirrer for 30 min at 50 °C. The black colour solution was obtained after that centrifuged and washed with water and ethanol, dry in the oven at 60 °C overnight. The obtained black powder is denoted as Ni nanoparticles which are further characterized by using XRD and TEM [24,25].

5.2.3 Functionalization of MWCNT

The MWCNT was functionalized before further use for Ni-Pd bimetallic nanocomposite. Chemical functionalization of the MWCNTs was accomplished by sonicating a combination of concentrated sulfuric and nitric acid (a ratio of 3:1) for 2 h at 40 °C. Now filtered and washed with double distilled water until pH 7.0 and the obtained material was dry in the oven at 100 °C overnight and represented as f-MWCNT. Functionalization increases solubility and reactivity [26].

5.2.4 Synthesis of Ni-Pd bimetallic nanoparticles decorated on f-MWCNT

The palladium nickel bimetallic nanoparticles have been synthesized by wet chemical reduction pathways. First of all, prepared a methanolic solution of K_2PdCl_4 (10 mM), 1% PVP solution, and 3-APTMS (0.5 and 5.4 M) solution. Take 400 µl K_2PdCl_4, 80 µl PVP, 100 µl f-MWCNT(1mg/ml) 3mg Ni NPs, and 80 µl 3-APTMS, mix them in a glass vial, and kept it in the oven at 40-45 °C for 60-70 s. The black colour solution was obtained which is centrifuged and dry in the oven overnight represented as Ni-Pd/f-MWCNT and confirmed by characterization.

5.2.5 Preparation of Ni-Pd/f-MWCNT/Fcmc modified electrode

The modified electrode was prepared by mixing the Ni-Pd/f-MWCNT nanocomposite with Fcmc and graphite in a mortar pestle. Nujol oil was added to make the paste of the material. The obtained paste was filled into a glass capillary which is connected with the copper wire. Fcmc/CPE and Ni NPs/CPE were also prepared for comparisons using the same techniques. The composition of materials used for electrode fabrication is shown in **Table 5.1**.

Table 5.1 Composition of the mediator-modified electrode

System	Ferrocene monocarboxylic acid (Fcmc) (w/w%)	Ni NPs / Ni-Pd/f-MWCNT (w/w%)	Graphite (w/w%)	Nujol oil (w/w%)
Fcmc /CPE	2.5	-	67.5	30
Ni NPs /CPE	2.5	0.3	67.2	30
Ni-Pd/f-MWCNT /CPE	2.5	0.3	67.2	30

5.2.6 Electrochemical Characterization

A Rigaku Miniflex 600 Desktop X-Ray Diffraction System using Cu Kα radiation was used to assess the nanocomposite's crystal structures. Carl Zeiss Microscopy LTD, EVO - Scanning Electron Microscope MA15 / 18 and Tecnai G2 20 TWIN transmission electron microscopy (TEM) were used to examine the surface morphology and particle size of the samples. Model-K-Alpha, Thermo Fisher Scientific XPS analysis was used to confirm the presence of elemental composition and their oxidation state. AFM was used to check the topography image of materials. Cyclic voltammetry, electrochemical impedance spectroscopy, and amperometry were all conducted using a standard three-electrode setup and a CHI 608C workstation. The phosphate buffer solution (PBS) of pH 7.0 was used as working electrolyte. The working electrode was a modified carbon paste electrode (CPE), while the counter and reference electrodes were composed of platinum foil (1 cm^2) and silver-silver chloride, respectively.

5.3 Results and Discussion

5.3.1 Materials characterization

X-ray diffraction analysis was used to learn more about the composition and structure of Ni-Pd/f-MWCNT nanocomposite. In **figure 5.1**, the peak 2θ = 44.4°, 51.6°, and 76.4° in the powder XRD corresponding to the Ni nanoparticles and the peak 2θ value 40°, 46.4°, 68.1° and 25.9° corresponding to the Pd NPs and f-MWCNT, respectively is depicted.

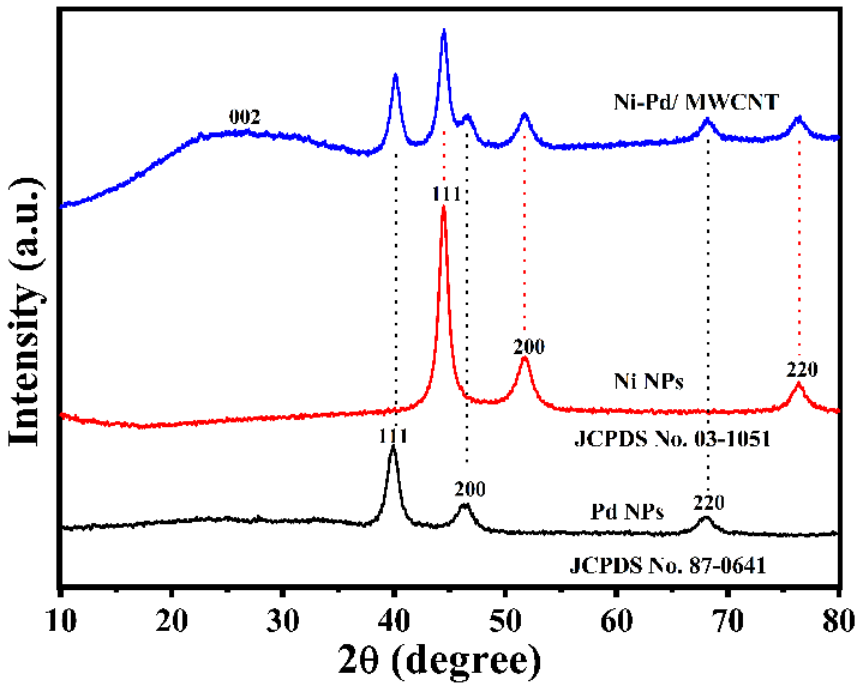

Figure 5.1 PXRD analysis of synthesized materials.

The XPS response of the bimetallic Ni-Pd/MWCNT nanocomposite is depicted in **figure 5.2 (a-c),** which includes information about the elemental composition, electronic structure and oxidation states of the material. **Figure 5.2 (a-c)** shows high-resolution XPS images of the core levels of Ni 2p, Pd 3d, and C 1s. In **figure 5.2 (b)**, we can see the Pd 3d spectrum, which reveals two distinct chemical states for Pd.

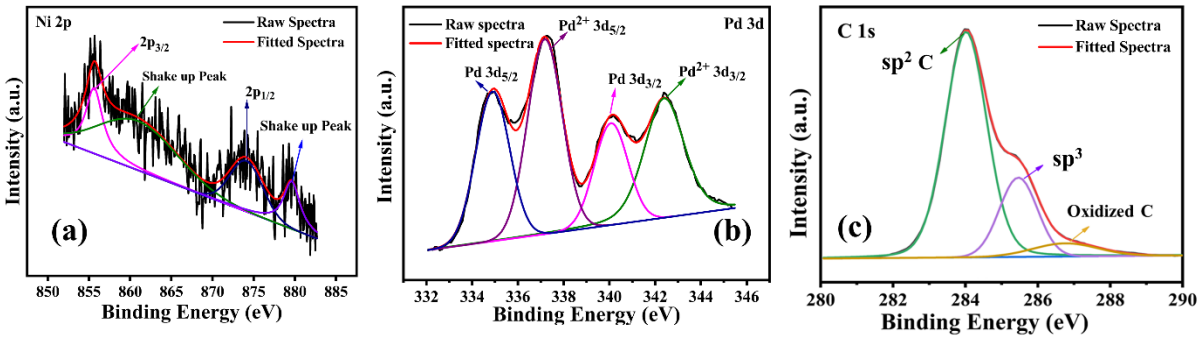

Figure 5.2 XPS data of nanocomposite Ni-Pd/f-MWCNT (a) Ni 2p, (b) Pd 3d, (c) C1s

The lower binding energy component might be attributed to metallic Pd, whereas the larger binding energy component show that a little amount of Pd is in oxidation state due to the surface oxidation, which is common in metallic nanomaterials [27–30].

The FE-SEM image of Ni-Pd/f-MWCNT were shown at high magnification in **figure 5.3**. The EDX and elemental colour mapping was used for the composition present in composite materials. A network of f-MWCNTs decorated with a large number of Ni-Pd nanoparticles became apparent, evidencing the tight entanglement of the Ni-Pd and the f-MWCNTs.

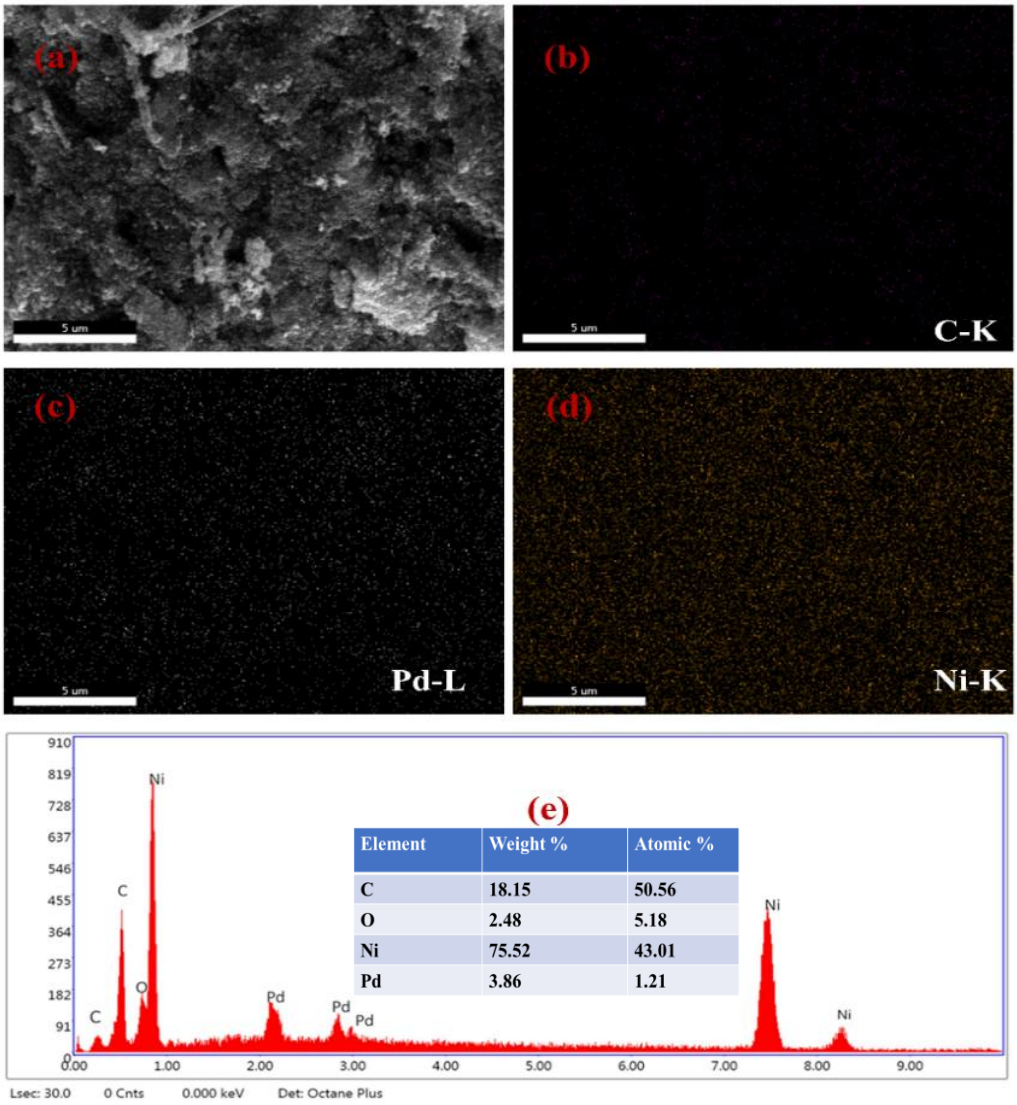

Figure 5.3 FE- SEM (a), elemental mapping (b, c, d) and EDX analysis (e) of synthesized composite nanomaterials (Ni-Pd/f-MWCNT).

Through TEM investigation, structure and size of Ni NPs and Ni-Pd/f-MWCNT were examined. Ni nanoparticles are found to have average particle size 30±5 nm and observed in aggregated form as shown **figure 5.4 (a)**. **Figure 5.4 (b)** shows the presence of nickel and palladium nanoparticles decorated on f-MWCNT. Figure 5.4(c, d) SAED image reveals the crystalline nature of the synthesized materials.

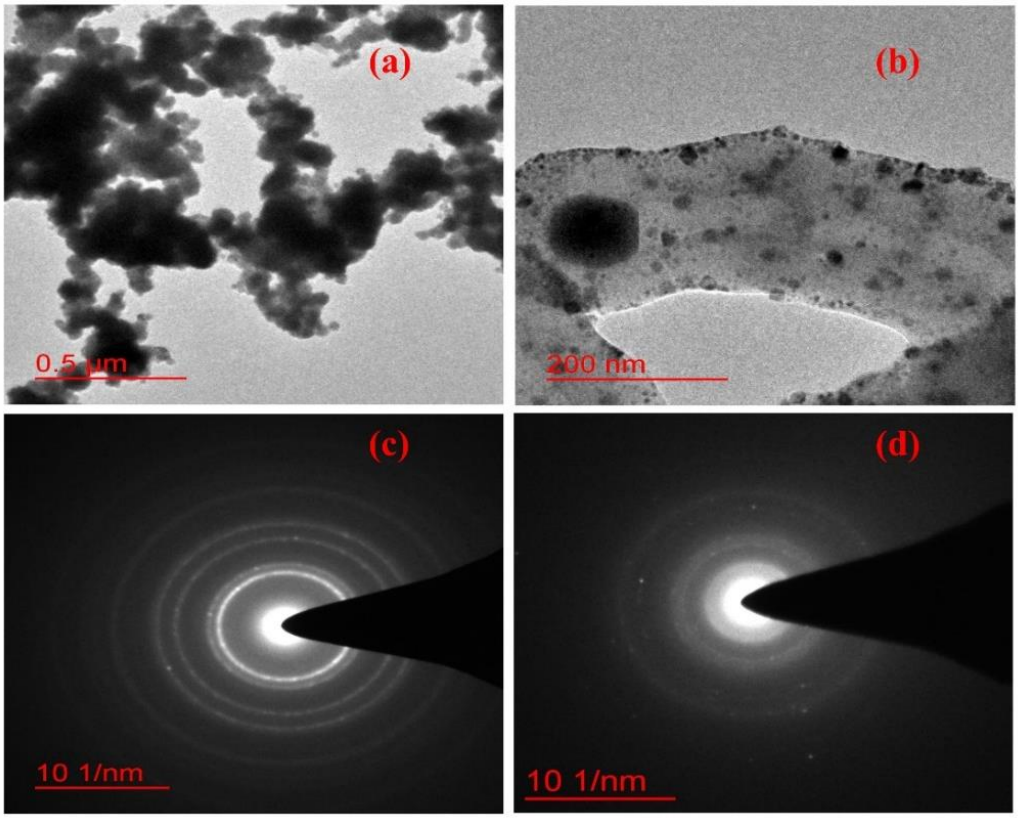

Figure 5.4 TEM analysis of (a) Ni NPs, and (b) Ni-Pd/ f-MWCNT. SAED Pattern (c) Ni NPs, and (d) Ni-Pd/ f-MWCNT

The topographic image before and after the electrochemical study of the modified electrode was carried out using atomic force spectroscopy (AFM) as shown in **figure 5.5**. From the figure 5.5, it is found that the surface roughness was around 1.481 nm and 1.593 nm before and after electrochemical sensing, respectively. There was an insignificant change in roughness which

confirms that the modified electrodes with Pd–Ni/f-MWCNT/CPE reveal the better stability toward DA determination [31].

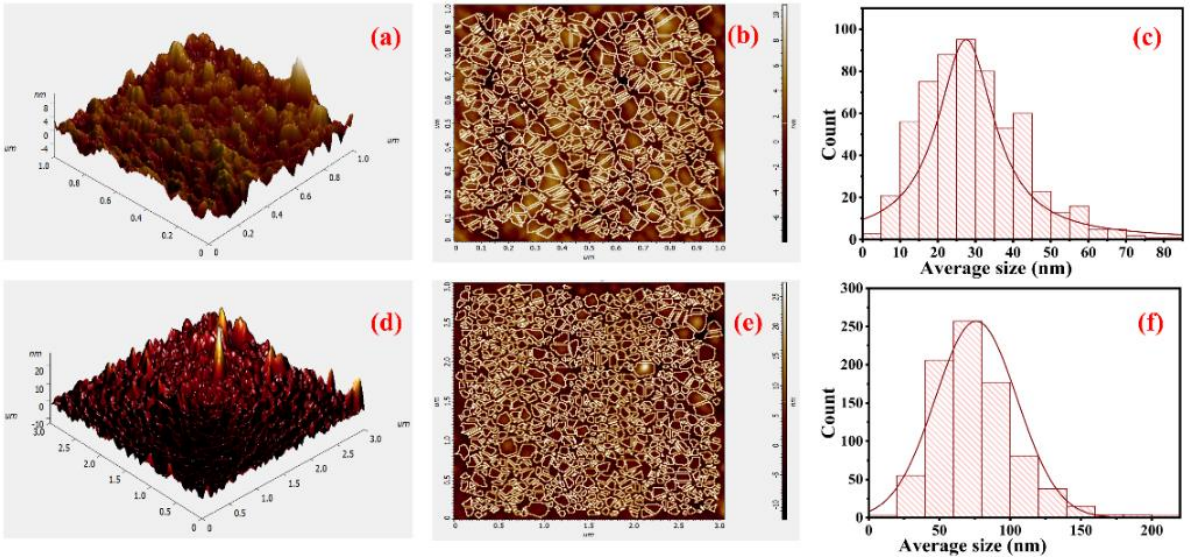

Figure 5.5 Atomic force spectroscopy image of Ni-Pd/f-MWCNT thin film before (a, b, c) and after electrochemical study (d, e, f).

5.3.2 Electrochemical studies

5.3.2.1 Voltammetric study of modified carbon paste electrode

In order to evaluate the analytical potential of the proposed electrochemical sensor, the CV, EIS, DPV, and amperometric techniques were used. Cyclic voltammetry was used to study the redox behavior of Fcmc using nanomaterials modified electrode in 0.1 M PBS (pH 7.0), the cyclic voltammograms (CVs) of the Fcmc/CPE, Fcmc/Ni/CPE, and Fcmc/Ni-Pd/f-MWCNT/CPE are shown in **figure 5.6**. It was found that all electrodes exhibited a pair of reversible redox peaks. A decrease in shifting of peak potential has been observed on moving from bare to modified electrode. The findings supported a decrease in difference between the anodic and cathodic peak potentials from 305 to 246 mV which correspond to better electrochemical behavior of the modified electrode.

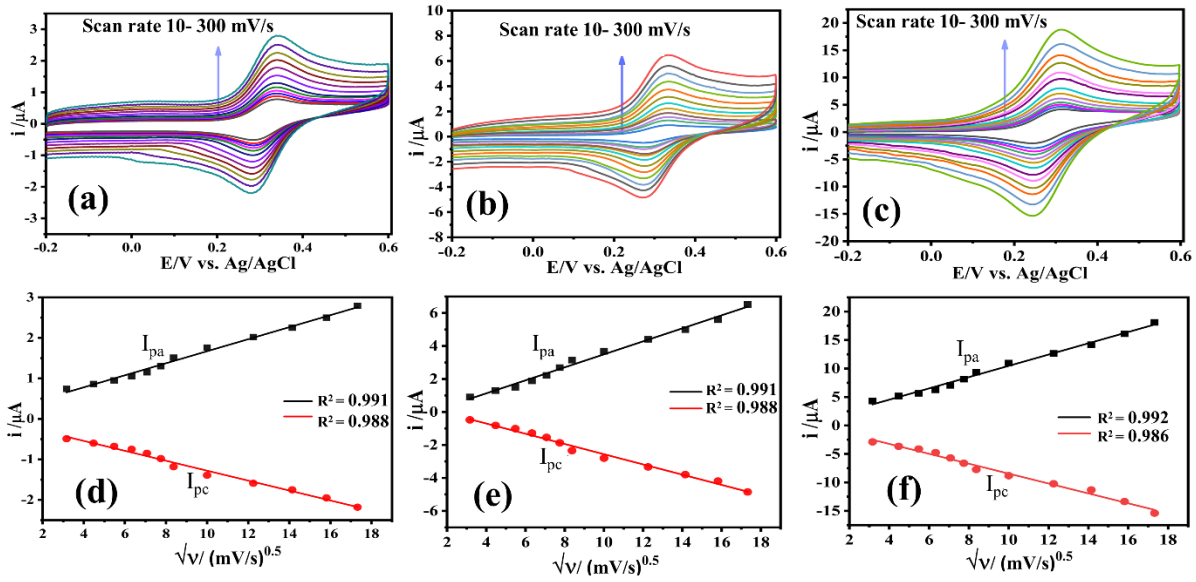

Figure 5.6 Cyclic voltammetric response and plot between the peak current vs square root of scan rates for electrodes (a, d) Fcmc/CPE, (b, e) Fcmc-Ni NPs/CPE, (c, f) Fcmc-Ni-Pd/f-MWCNT/CPE, respectively.

Cyclic voltammograms were also obtained after the addition of DA. For comparison, cyclic voltammetric data of before and after addition of dopamine is shown in **figure 5.7.** When compared to the Fcmc-Ni/CPE, the Fcmc-Ni-Pd/f-MWCNT/CPE exhibited the highest DA oxidation peak current, demonstrating the excellent electrocatalytic activity of modified electrodes for DA oxidation. The enhancement in the peak current is ascribed to the synergistic effects between the Pd–Ni bimetallic nanoparticles doped on f-MWCNT and Fcmc.

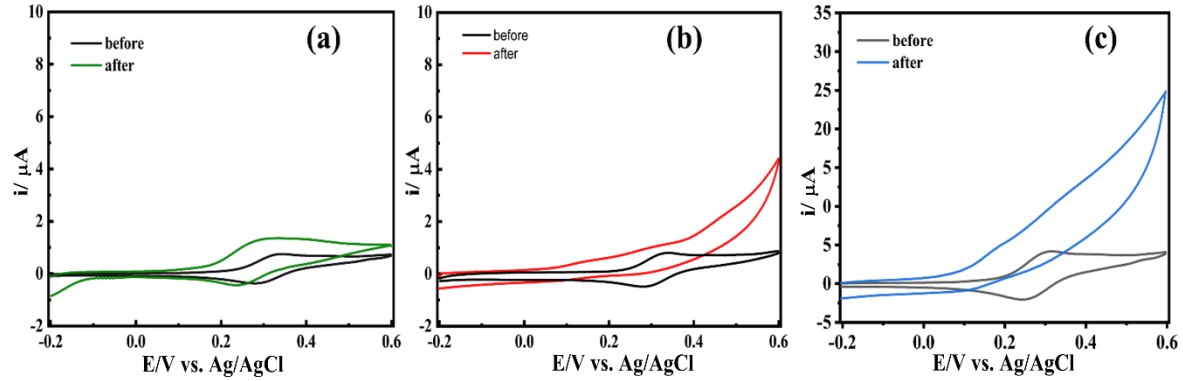

Figure 5.7 Cyclic voltammetric study before and after dopamine (100 mM) addition at 10 mV/s under similar condition, (a) Fcmc /CPE, (b) Ni NPs /CPE, and (c) Ni-Pd /f-MWCNT/CPE, respectively.

The data has been correlated using Randles-Sevcik equation (eq. 1) for the redox process and reaction was found to be diffusion controlled [32].

$$I_p = 2.69 \times 10^5 n^{3/2} A\ C\ D^{1/2}\ v^{1/2} \qquad (1)$$

According to equation (2), a rough estimate of the electrode's surface coverage might be determined [33]. $I_p = n^2F^2A\ v\ \Gamma/4RT$ (2)

Here, n represent the number of electrons involved, I_p is the peak current, A is the geometrical surface area of CPE (0.031 cm^2), ν is the scan rate (100 mV/s), F is the Faraday constant, T is the temperature and R denote the universal gas constant.

The calculated Γ values for modified electrodes are revealed in **Table 5.2** shown below.

Table 5.2 Electrode's surface coverage (Γ)

Modified electrodes	Γ (mol /cm^2)
Fcmc/CPE	0.6231 x 10^{-9}
Fcmc-Ni NPs/CPE	1.3167 x 10^{-9}
Fcmc-Ni-Pd/f-MWCNT	3.8560 x 10^{-9}

Further, impedance spectroscopy verified that the decreased charge transfer resistance as electrode modified with Ni-Pd/f-MWCNT nanocomposite was seen while the anodic and cathodic peak currents were continuously elevated under identical conditions.

5.3.3 EIS Study

Electrochemical impedance spectroscopy is a convenient, versatile, and non-destructive technique that provides valuable information about the electrochemical behavior and surface characteristics of electrodes, both bare and modified. The electrochemical impedance measurement for the modified electrodes, Fcmc/CPE, Ni NPs/CPE, and Ni-Pd/f-MWCNT/CPE were performed using 0.1M PBS pH 7.0 under similar conditions. The experimental data was best fitted on a model RC(RW) circuit. The charge-transfer resistance (R_{ct}) at the interface is shown by the semicircle's diameter in the Nyquist plot. The modified electrode Ni-Pd/f-MWCNT possessed the lowest semicircle diameter on the Nyquist plots, which indicated a lower R_{ct} value for this electrode. As a result, it can transmit electrons more effectively than Ni NPs modified and bare electrodes. It reveals that Ni-Pd /f- MWCNT composite-modified electrode could reduce the R_{ct} value and boost the electron transfer phenomena. Figure 5.8 shows Nyquist plots at different concentrations of DA, which were used to calculate the values of R_{ct} under similar condition.

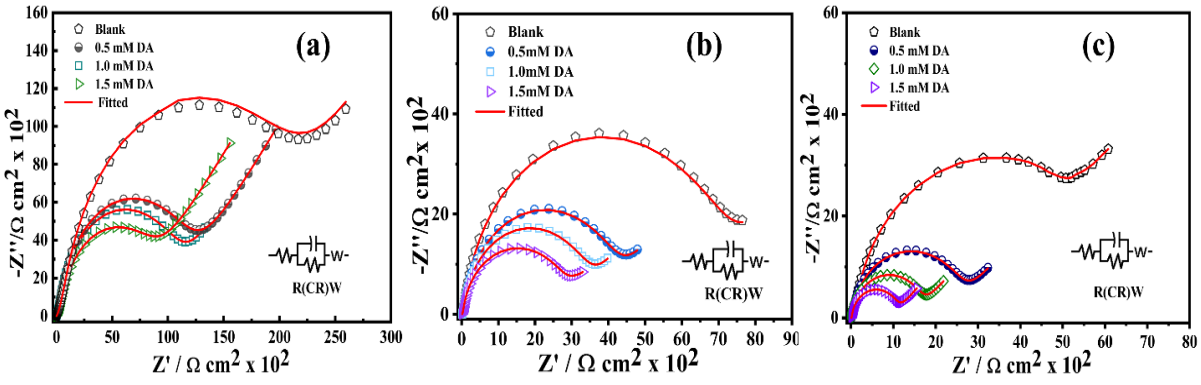

Figure 5.8 EIS study for modified electrodes under similar conditions (a) Fcmc /CPE, (b) Ni NPs /CPE, and (c) Ni-Pd /f-MWCNT /CPE, respectively.

The R_{ct} value for bare electrodes, Ni NPs, and Ni-Pd/f-MWCNT composite-modified electrodes are shown in **Table 5.3**.

Table 5.3 Calculated charge transfer resistance (R_{ct}) value of the modified electrodes at various concentrations of dopamine.

Concentration	**Modified electrodes**		
	Fcmc /CPE (R_{ct} kΩ cm^2)	**Ni NPs /CPE** (R_{ct} kΩ cm^2)	**Ni-Pd /f-MWCNT /CPE** (R_{ct} kΩ cm^2)
Blank	27.17	8.04	6.32
0.5 mM DA	15.82	4.77	3.05
1.0 mM DA	13.89	3.95	2.01
1.5 mM DA	12.43	3.15	1.21

5.3.4 Differential pulse voltammetry (DPV)

Ni-Pd/f-MWCNT composite current responses to DA detection in 0.1 M PBS were studied using DPV. As can be seen in **figure 5.9 (a, b, c)**, the oxidative peak intensity of DPV steadily rises as DA concentration is increased. These findings demonstrate that the Ni-Pd/f-MWCNT electrode is very sensitive to the measurement of DA and has outstanding electrocatalytic activity. In **figure 5.9** (c) shows the slight shifting in peak potential which is good correlation for enhancing the sensing of dopamine. **Figure 5.9 (d)** reveals the plot of current vs concentration of dopamine with correlation coefficient for all three electrodes. The linear equation $Ip = 0.0438\ [C]\ \mu M + 1.476$ provides strong linear interactions between the peak current and the concentration of DA for the Ni-Pd/f-MWCNT modified electrode.

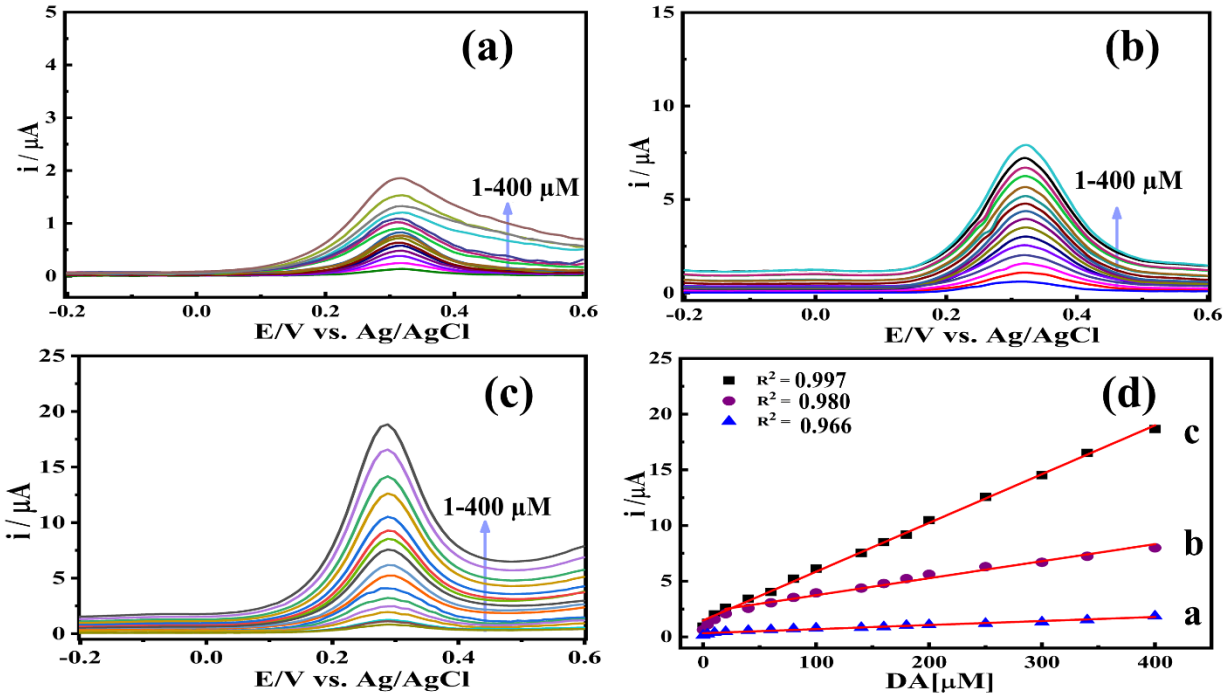

Figure 5.9 DPV analysis under similar condition for all modified electrodes (a) Fcmc /CPE, (b)Ni-NPs /CPE, (c) Ni-Pd/f-MWCNT /CPE, and (d) plot of current vs concentration study for modified electrode.

5.3.5 Amperometry i-t curves study

Constant potential amperometry was used to analyze the efficiency of the modified carbon paste electrodes incorporating Ni NPs, and Ni-Pd/f-MWCNT. The amperometric responses of the modified Fcmc/CPE electrodes at +0.28 V (vs. Ag/AgCl in PBS) were studied in order to acquire several sensor parameters such as linear range, sensitivity, low detection limit (LOD), and repeatability. DA was added progressively at various concentration ranges. The modified electrode with Ni-Pd/f-MWCNT reveals a high i-t current than others, as shown in **figure 5.10**. When DA was added to PBS, the current responses stabilized in less than 5s. The amperometric responses were used to create a calibration plot, which shows that the current response increased linearly with increasing DA concentrations **(figure 5. 10)**.

It is common practice to employ these techniques, which involve recording the current response between the working electrode and the counter electrode, to make a quantitative determination.

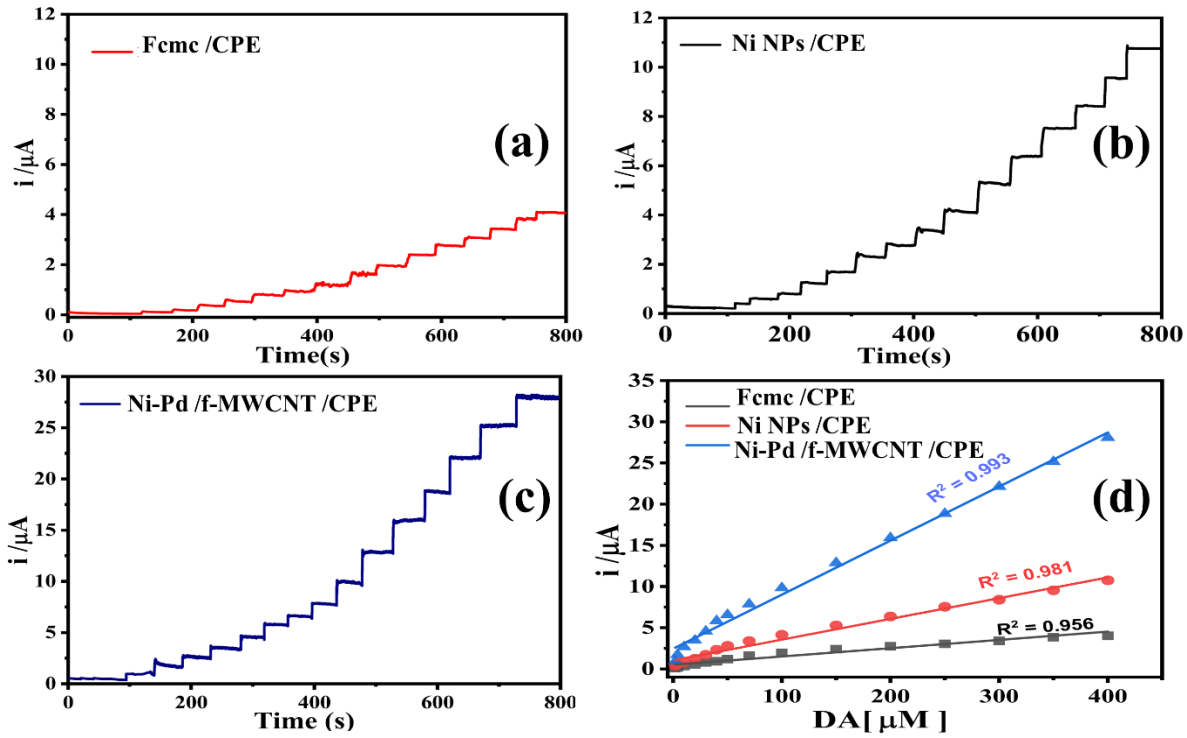

Figure 5.10 Amperometric i-t curve for (a) Fcmc/CPE, (b) Ni NPs/CPE, (c) Ni-Pd/f-MWCNT modified electrodes under similar condition and (d) their current vs concentration plot.

Advantages of the amperometric approach include its ability to detect at extremely low concentrations, its excellent sensitivity and selectivity, and its compact size. By minimizing the capacitance current, the amperometric approach outperforms the CV techniques in terms of sensitivity. Since the electrode surface was changed with Ni NPs, which improved electrical conductivity and increased efficient area, the redox current of the Ni-Pd/ f-MWCNT modified sensor spontaneously increased. Due to the increased electroactive surface area (EASA) and strong electron conductivity of Ni-Pd/f-MWCNT, which offers more active sites for the electrochemical reaction, the DA oxidation peak current of the Fcmc-Ni-Pd/f-MWCNT/CPE

improves. A high electroactive surface area (EASA) surface facilitates the electron transfer reaction during the electrochemical detection of DA.

The linearity is shown by the calibration plot, and the regression coefficient (R^2) for DA concentrations between 2 µM and 400 µM obtained from the fitting equation (Eq. (3)) is 0.993.

$$I_p = 0.0656[C]\ \mu M + 2.4541 \qquad (3)$$

Where C is the concentration of dopamine.

To calculate the limit of detection (LOD) and limit of quantification (LOQ), for dopamine sensing the following equations (Eqs. (4) and (5)) were applied [34].

$$LOD = \frac{3S}{M} \qquad (4)$$

$$LOQ = \frac{10S}{M} \qquad (5)$$

5.3.6 Reproducibility, selectivity, and stability

The Ni-Pd/f-MWCNT nanocomposite material has been evaluated to demonstrate the advantages of this sensor by analysing the reproducibility, repeatability, and stability of the produced electrode. The reproducibility of the Ni-Pd/f-MWCNT modified electrode tested in 0.1 M PBS (pH = 7.0) using the amperometric method is shown in **figure 5.11 (a)** (the electrode is newly produced for each individual test). The amperometric studies were carried out five times under similar conditions, and the i-t curves for all five electrodes show almost similar currents with a relative standard deviation (RSD) of 2.31%, demonstrating the electrochemical sensor's high reproducibility. The DPV technique was also used to examine the cycle stability

of the modified electrode Ni-Pd/f-MWCNT. The outstanding durability of the Ni-Pd/f-MWCNT modified sensor is demonstrated by **figure 5.11 (b),** which indicates that DPV properties for DA, such as peak currents and an integral area of DPV curves, remain unaltered after 20 cycles.

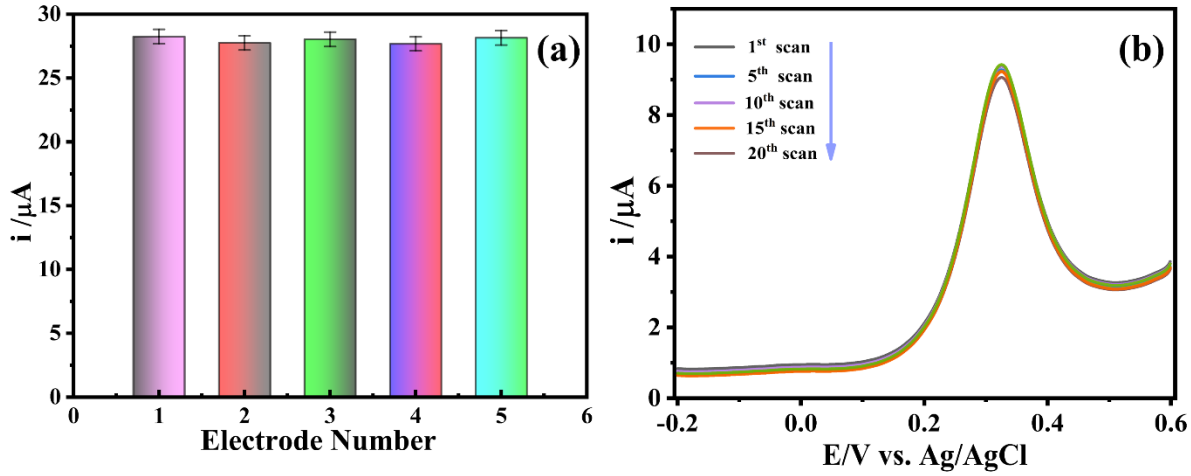

Figure 5.11 (a) Reproducibility and **(b)** stability of Ni-Pd/f-MWCNT electrodes for detection of DA

The results reported here revealed the remarkable reproducibility, repeatability, and stability of the Ni-Pd/f-MWCNT nanocomposite sensor for the electrochemical detection of dopamine. The Ni-Pd/f-MWCNT fabricated sensor can produce better or equivalent results for detecting DA when compared to the earlier findings (**Table 5.4**).

Table 5.4 Comparison between the proposed and reported sensor

Modified electrodes	**Analytical technique**	**Linear range (µM)**	**LOD (µM)**	**Reference**
Pd/CeO_2/rGO/ GCE	DPV	5-240	0.69	[34]
AuPd@Fe_2O_3 NPs/GCE	Chronoamperometry	0.01-832	0.01	[35]
Au NPs/MoS_2/nanocomposite	DPV	1-500	0.1	[36]
TCNQ@$CoWO_4$/CPE	Amperometry	2-80	4.55	[37]
Au/Cu_2O/rGO	DPV	10-90	3.90	[38]
Au-SiO_2 / GCE	DPV	10-500	1.98	[39]
pGr-MWCNT/Au	DPV	1-100	0.07	[40]
3D rGO/MWCNTS/ZrFeOx/GCE	DPV	1-12 12-180	0.23	[41]
CQDs/ CuO	SWV	1-180	25.40	[42]
Ag-Cu decorated/ ZnO-NFLCs	Amperometry	0.1-10	0.21	[43]
CTAB-GO/MWCNT/GCE	DPV	5-500	1.5	[44]
H-Co-Ni-/GCE	DPV	10-500	8	[45]
Poly SCCy/ PdNPs/CPE	DPV	5-100	1.87	[46]
Ni-Pd/f-MWCNT/CPE	**Amperometric & DPV**	**2-400**	**0.05**	**This work**

pGr: 3,4,9,10-perylene tetracarboxylic acid-graphene, CQDs; carbon quantum dots, SCCy; solochrome cyanine, NFLCs; nanoflower like composite

5.3.7 Interferences study and effect of pH

The anti-interference characteristics of the fabricated Ni-Pd/f-MWCNT/CPE sensor were evaluated using amperometry in the presence of possible interference species. The amperometric response to several interferences that occur frequently during DA detection was

recorded to assess the sensitivity of the proposed sensor to such interferences i.e., AA, UA, NaCl, and KCl shown in **figure 5.12 (a)**.

The amperometry study have been carried out at different pH values (pH 6 to 8) PBS (0.1 M) for the modified electrode**.** We obtained the maximum oxidation current at pH 7 during study. As a result of this pH 7.0 is considered as optimize pH value to detect the DA as shown in **figure 5.12 (b).**

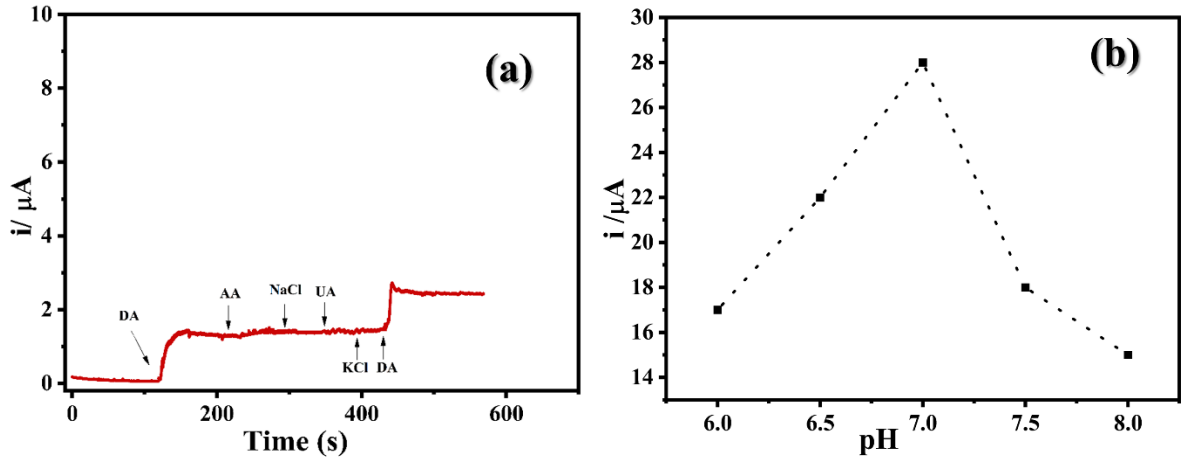

Figure 5.12 (a) Interference study (b) Amperometric response at different pH

5.3.8 Real sample analysis

The amperometry approach was used to evaluate the feasibility, accuracy, and sensitivity of the constructed Ni-Pd/f-MWCNT/CPE with a commercially available dopamine hydrochloride (DA-HCl) injection. As a first step in preparing the DA sample, the commercial dopamine injection was diluted with distilled water. **Table 5.5** shows the concentrations of DA that were added to 0.1 M PBS solution (pH = 7.0) for the analysis of actual samples. The recovery rate is usually calculated by dividing the concentration under test by the concentration that was added. In the context of an electrochemical sensor used for dopamine sensing, the recovery rate refers to the accuracy with which the sensor can detect and quantify dopamine in a sample. Specifically, it measures the sensor's ability to recover the known amount of dopamine added

to a sample during testing. Based on the results in **Table 5.5**, the fabricated sensor demonstrates robust reliability for the determination of dopamine in real samples, with recovery rates ranging from 97.75% to 101.0%. These values indicate that the sensor performs within an acceptable accuracy range for practical applications. These findings demonstrate the viability of Ni-Pd/f-MWCNT/CPE as a suitable electrode for the detection of DA in actual samples.

Table 5.5 Recovery rate results of DA in real sample.

Sample	Added (µM)	Found (µM)	Recovery (%)
1	10	10.10	101.0
2	20	19.75	98.75
3	40	39.10	97.75
4	60	59.5	99.16

5.4 Conclusions

The given results are significant because they provide evidence for the viability of DA detection utilizing electrodes acquired using a very straightforward, low-cost preparation process with short fabrication timeframes. For quantitative DA sensing, the produced modified electrode Ni-Pd/f-MWCNT/CPE was shown to have sterling electrochemical performance. The C_{dl} values for Fcmc /CPE, Ni NPs /CPE, and Ni-Pd /f-MWCNT/CPE were 0.112 µF, 0.754 µF, and 1.612 µ F, respectively. The modified sensor showed remarkable results in terms of sensitivity, selectivity, and electrocatalytic activity, including a linear response to dopamine concentrations of 2 - 400 µM, a detection limit of 0.05 µM, LOQ 0.166 µM, sensitivity 2.116 µA/µMcm^2 and excellent recoveries of 99% following dopamine injection. For dopamine detection in biological studies, the Ni-Pd/f-MWCNT nanocomposite might serve as a powerful alternative catalyst.

5.5 References

[1] D. Kim, S. Lee, Y. Piao, Electrochemical determination of dopamine and acetaminophen using activated graphene-Nafion modified glassy carbon electrode, *J. Electroanal. Chem.*, **794** (2017): 221–228. https://doi.org/10.1016/j.jelechem.2017.04.018.

[2] M. Wei, Y. Qiao, H. Zhao, J. Liang, T. Li, Y. Luo, S. Lu, X. Shi, W. Lu, X. Sun, Electrochemical non-enzymatic glucose sensors: recent progress and perspectives, *Chem. Commun.*, **56** (2020): 14553–14569. https://doi.org/10.1039/d0cc05650b.

[3] J. Feng, Q. Li, J. Cai, T. Yang, J. Chen, X. Hou, Electrochemical detection mechanism of dopamine and uric acid on titanium nitride-reduced graphene oxide composite with and without ascorbic acid, *Sens. Actuators B: Chem.*, **298** (2019): 126872. https://doi.org/10.1016/j.snb.2019.126872.

[4] R. Sha, N. Vishnu, S. Badhulika, MoS_2 based ultra-low-cost, flexible, non-enzymatic and non-invasive electrochemical sensor for highly selective detection of Uric acid in human urine samples, *Sens. Actuators B: Chem.*, **279** (2019): 53–60. https://doi.org/10.1016/j.snb.2018.09.106.

[5] L.Q. Xie, Y.H. Zhang, F. Gao, Q.A. Wu, P.Y. Xu, S.S. Wang, N.N. Gao, Q.X. Wang, A highly sensitive dopamine sensor based on a polyaniline/reduced graphene oxide/Nafion nanocomposite, *Chin. Chem. Lett.* **28** (2017): 41–48. https://doi.org/10.1016/j.cclet.2016.05.015.

[6] T. Kokulnathan, T.J. Wang, E.A. Kumar, N. Duraisamy, An-Ting Lee, An electrochemical platform based on yttrium oxide/boron nitride nanocomposite for the detection of dopamine, Sens. Actuators B: Chem., **349** (2021): 130787. https://doi.org/10.1016/j.snb.2021.130787.

[7] C. Wang, J. Chen, L. Zhang, Y. Yang, M. Huang, C. Chen, C. Li, Y. Xie, P. Zhao, J. Fei, An ultra-sensitive dopamine photoelectrochemical sensing platform based on two-dimensional Zn carbon nanosheets, hollow Cu_2O and CdTe QDs composite films, *Carbon*, **198** (2022) 101–109. https://doi.org/10.1016/j.carbon.2022.07.007.

[8] B. Patella, A. Sortino, F. Mazzara, G. Aiello, G. Drago, C. Torino, A. Vilasi, A. O'Riordan, R. Inguanta, Electrochemical detection of dopamine with negligible interference from ascorbic and uric acid by means of reduced graphene oxide and metals-NPs based electrodes, *Anal. Chim. Acta*, **1187** (2021): 339124. https://doi.org/10.1016/j.aca.2021.339124.

[9] L.O. Orzari, M.H.M.T. Assumpção, J. Nandenha, A.O. Neto, L.H.M. Junior, M. Bergamini, B.C. Janegitz, Pd, Ag and Bi carbon-supported electrocatalysts as electrochemical multifunctional materials for ethanol oxidation and dopamine determination, *Electrochim. Acta*, **428** (2022): 140932. https://doi.org/10.1016/j.electacta.2022.140932.

[10] H. Ouyang, W. Li, Y. Long, Carbon-doped h-BN for the enhanced electrochemical determination of dopamine, *Electrochim. Acta*, **369** (2021): 137682. https://doi.org/10.1016/j.electacta.2020.137682.

[11] A. Arroquia, I. Acosta, M.P.G. Armada, Self-assembled gold decorated polydopamine nanospheres as electrochemical sensor for simultaneous determination of ascorbic acid, dopamine, uric acid and tryptophan, *Mater. Sci. Eng. C*, **109** (2020): 110610. https://doi.org/10.1016/j.msec.2019.110602.

[12] A. Savk, B. Özdil, B. Demirkan, M.S. Nas, M.H. Calimli, M.H. Alma, Inamuddin, A.M. Asiri, F. Şen, Multiwalled carbon nanotube-based nanosensor for ultrasensitive detection of uric acid, dopamine, and ascorbic acid, *Mater. Sci. Eng. C*, **99** (2019): 248–254. https://doi.org/10.1016/j.msec.2019.01.113.

[13] Y.H. Chang, P.M. Woi, Y. Alias, The selective electrochemical detection of dopamine in the presence of ascorbic acid and uric acid using electro-polymerised-β-cyclodextrin incorporated f-MWCNTs/polyaniline modified glassy carbon electrode, *Microchem. J.*, **148** (2019): 322–330. https://doi.org/10.1016/j.microc.2019.04.081.

[14] K. Kaewket, C. Karuwan, S. Sonsupap, S. Maensiri, K. Ngamchuea, Anti-Fouling Effects of Carbon Nanofiber in Electrochemical Sensing of Phenolic Compounds, *J. Electrochem. Soc.*, **168** (2021): 067501. https://doi.org/10.1149/1945-7111/ac0358.

[15] B.L. Hanssen, S. Siraj, D.K.Y. Wong, Recent strategies to minimise fouling in electrochemical detection systems, *Rev. Anal. Chem.*, **35** (2016): 1–28. https://doi.org/10.1515/revac-2015-0008.

[16] E. Peltola, S. Sainio, K.B. Holt, T. Palomäki, J. Koskinen, T. Laurila, Electrochemical Fouling of Dopamine and Recovery of Carbon Electrodes, *Anal. Chem.*, **90** (2018): 1408–1416. https://doi.org/10.1021/acs.analchem.7b04793.

[17] B. Liu, H. Guo, L. Sun, Z. Pan, L. Peng, M. Wang, N. Wu, Y. Chen, X. Wei, W. Yang, Electrochemical sensor based on covalent organic frameworks/MWCNT for simultaneous detection of catechol and hydroquinone, *Colloids Surf. A: Physicochem. Eng. Asp.*, **639** (2022): 128335. https://doi.org/10.1016/j.colsurfa.2022.128335.

[18] J. Cheng, X. Wang, T. Nie, L. Yin, S. Wang, Y. Zhao, H. Wu, H. Mei, A novel electrochemical sensing platform for detection of dopamine based on gold nanobipyramid/multi-walled carbon nanotube hybrids, *Anal. Bioanal. Chem.*, **412** (2020): 2433–2441. https://doi.org/10.1007/s00216-020-02455-5.

[19] G. Li, B. Yuan, L. Zhao, W. Gao, C. Xu, G. Liu, Fouling-resistant electrode for electrochemical sensing based on covalent-organic frameworks TpPA-1 dispersed cabon nanotubes, *Talanta*, **267** (2024): 125162. https://doi.org/10.1016/j.talanta.2023.125162.

[20] F. Heshmatpour, R. Abazari, Formation of dispersed palladium-nickel bimetallic nanoparticles in microemulsions: Synthesis, characterization, and their use as efficient heterogeneous recyclable catalysts for the amination reactions of aryl chlorides under

mild conditions, *RSC Adv.*, **4** (2014): 55815–55826. https://doi.org/10.1039/c4ra06958g.

[21] R.K. Shervedani, M. Karevan, A. Amini, Prickly nickel nanowires grown on Cu substrate as a supersensitive enzyme-free electrochemical glucose sensor, *Sens. Actuators B*: *Chem*. **204** (2014): 783–790. https://doi.org/10.1016/j.snb.2014.08.033.

[22] J.A.S.B. Cardoso, B. Šljukić, E. Kayhan, C.A.C. Sequeira, D.M.F. Santos, Palladium-nickel on tin oxide-carbon composite supports for electrocatalytic hydrogen evolution, *Catal. Today*, **357** (2020): 302–310. https://doi.org/10.1016/j.cattod.2019.05.056.

[23] Y. Zhang, Y. Liao, G. Shi, W. Wang, B. Su, Preparation, characterization, and catalytic performance of Pd-Ni/AC bimetallic nano-catalysts, *Green Process. Synth.*, **9** (2020): 760–769. https://doi.org/10.1515/gps-2020-0071.

[24] S. Liu, S.K. Tam, K.M. Ng, Dual-reductant synthesis of nickel nanoparticles for use in screen-printing conductive paste, *J. Nanoparticle Res.*, **23** (2021): 78. https://doi.org/10.1007/s11051-021-05191-8.

[25] M.R. Ahghari, V. Soltaninejad, A. Maleki, Synthesis of nickel nanoparticles by a green and convenient method as a magnetic mirror with antibacterial activities, *Sci. Rep.*, **10** (2020): 12627. https://doi.org/10.1038/s41598-020-69679-4.

[26] M.J. Huhn-Ibarra, M.I. Loría-Bastarrachea, S. Duarte-Aranda, A. de J. Montes-Luna, J. Ortiz-Espinoza, M.O. González-Díaz, M. Aguilar-Vega, PPSU dual layer hollow fiber mixed matrix membranes with functionalized MWCNT for enhanced antifouling, salt and dye rejection in water treatment, *J. Appl. Polym. Sci.* **139** (2022): e53203. https://doi.org/10.1002/app.53203.

[27] H. Cheng, N. Yang, G. Liu, Y. Ge, J. Huang, Q. Yun, Y. Du, C.J. Sun, B. Chen, J. Liu, H. Zhang, Ligand-Exchange-Induced Amorphization of Pd Nanomaterials for Highly Efficient Electrocatalytic Hydrogen Evolution Reaction, *Adv. Mater.*, **32** (2020): 1902964. https://doi.org/10.1002/adma.201902964.

[28] X.L. Cai, C.H. Liu, J. Liu, Y. Lu, Y.N. Zhong, K.Q. Nie, J.L. Xu, X. Gao, X.H. Sun, S.D. Wang, Synergistic effects in CNTs-Pd Au/Pt trimetallic nanoparticles with high electrocatalytic activity and stability, *Nanomicro. Lett.*, **9** (2017): 1–10. https://doi.org/10.1007/s40820-017-0149-1.

[29] M.G. Hosseini, F. Hosseinzadeh, P. Zardari, O. Mermer, Pd-Ni nanoparticle supported on reduced graphene oxide and multi-walled carbon nanotubes as electrocatalyst for oxygen reduction reaction, *Fuller. Nanotub. Carbon Nanostructures*, **26** (2018): 675–687. https://doi.org/10.1080/1536383X.2018.1465049.

[30] F. Gulbagca, A. Aygün, M. Gülcan, S. Ozdemir, S. Gonca, F. Şen, Green synthesis of palladium nanoparticles: Preparation, characterization, and investigation of antioxidant, antimicrobial, anticancer, and DNA cleavage activities, *Appl. Organomet. Chem.*, **35** (2021): e6272. https://doi.org/10.1002/aoc.6272.

[31] G. Dutta, F.C.B. Fernandes, P. Estrela, D. Moschou, P.R. Bueno, Impact of surface roughness on the self-assembling of molecular films onto gold electrodes for label-free biosensing applications, *Electrochim. Acta*, **378** (2021): 138137. https://doi.org/10.1016/j.electacta.2021.138137.

[32] A.J. Bard, L.R. Faulkner, H.S. White, Electrochemical methods: fundamentals and applications, *John Wiley & Sons*, 2022.

[33] X. Zheng, X. Zhou, X. Ji, R. Lin, W. Lin, Simultaneous determination of ascorbic acid, dopamine and uric acid using poly(4-aminobutyric acid) modified glassy carbon electrode, *Sens. Actuators B: Chem.*, **178** (2013): 359–365. https://doi.org/10.1016/j.snb.2012.12.115.

[34] G. Venkata Prasad, S.J. Jang, Y. Chandra Sekhar, T. Madhusudana Reddy, L. Subramanyam Sarma, H.B. Kim, T. Hyun Kim, Fine-tuning of Pd–CeO_2/rGO nanocomposite: A facile synergetic strategy for effective electrochemical detection of dopamine in pharmaceutical and biological samples, *J. Electroanal. Chem.*, **941** (2023): 117544. https://doi.org/10.1016/j.jelechem.2023.117544.

[35] M. Dai, Q. Zhu, D. Han, L. Niu, Z. Wang, Sensitive and selective electrochemical sensor for the detection of dopamine by using AuPd@Fe_2O_3 nanoparticles as catalyst, Adv. Sensor. Energy Mater., **2** (2023): 100048. https://doi.org/10.1016/j.asems.2023.100048.

[36] K.J. Huang, J.Z. Zhang, Y.J. Liu, L.L. Wang, Novel electrochemical sensing platform based on molybdenum disulfide nanosheets-polyaniline composites and Au nanoparticles, *Sens. Actuators B: Chem.*, **194** (2014): 303–310. https://doi.org/10.1016/j.snb.2013.12.106.

[37] K.K. Maurya, K. Singh, M. Malviya, Fabrication of dopamine sensor based on a carbon paste electrode modified with tetracyanoquinodimethane and cobalt tungstate nanoparticles, J. *Mater. Sci.: Mater. Electron.*, **35** (2024): 13. https://doi.org/10.1007/s10854-023-11721-y.

[38] T.K. Aparna, R. Sivasubramanian, M.A. Dar, One-pot synthesis of Au-Cu_2O/rGO nanocomposite based electrochemical sensor for selective and simultaneous detection of dopamine and uric acid, *J. Alloys Compd.*, **741** (2018): 1130–1141. https://doi.org/10.1016/j.jallcom.2018.01.205.

[39] S. Immanuel, T.K. Aparna, R. Sivasubramanian, A facile preparation of Au—SiO_2 nanocomposite for simultaneous electrochemical detection of dopamine and uric acid, *Surf. Interfaces*, **14** (2019): 82–91. https://doi.org/10.1016/j.surfin.2018.11.010.

[40] C. Zhang, J. Ren, J. Zhou, M. Cui, N. Li, B. Han, Q. Chen, Facile fabrication of a 3,4,9,10-perylene tetracarboxylic acid functionalized graphene-multiwalled carbon nanotube-gold nanoparticle nanocomposite for highly sensitive and selective electrochemical detection of dopamine, *Analyst*, **143** (2018): 3075–3084. https://doi.org/10.1039/c8an00559a.

[41] A. Xie, H. Wang, J. Lin, J. Pan, M. Li, J. Wang, S. Jiang, S. Luo, 3D rGO/MWCNTs-loaded bimetallic-organic gel derived $ZrFeO_x$ as an electrochemical sensor for simultaneous detection of dopamine and paracetamol, *J. Alloys Compd*., **938** (2023): 168647. https://doi.org/10.1016/j.jallcom.2022.168647.

[42] S.E. Elugoke, O.E. Fayemi, A.S. Adekunle, B.B. Mamba, T.T.I. Nkambule, E.E. Ebenso, Electrochemical sensor for the detection of dopamine using carbon quantum dots/copper oxide nanocomposite modified electrode, *FlatChem*, **33** (2022): 100372. https://doi.org/10.1016/j.flatc.2022.100372.

[43] S. Ponnada, D.B. Gorle, M.S. Kiai, S. Rajagopal, R.K. Sharma, A. Nowduri, A facile, cost-effective, rapid, single-step synthesis of Ag-Cu decorated ZnO nanoflower-like composites (NFLCs) for electrochemical sensing of dopamine, *Mater*. *Adv*., **2** (2021): 5986–5996. https://doi.org/10.1039/d1ma00319d.

[44] Y.J. Yang, W. Li, CTAB functionalized graphene oxide/multiwalled carbon nanotube composite modified electrode for the simultaneous determination of ascorbic acid, dopamine, uric acid and nitrite, *Biosens*. *Bioelectron*., **56** (2014): 300–306. https://doi.org/10.1016/j.bios.2014.01.037.

[45] C. Yang, X. Sun, C. Zhang, M. Liu, Green synthesis of Co-Ni hollow spheres for its electrochemical detection of dopamine, *J*. *Nanoparticle Res*., **22** (2020): 55. https://doi.org/10.1007/s11051-020-4775-z.

[46] K. Reddaiah, T.M. Reddy, K. Mallikarjuna, G. Narasimha, Electrochemical detection of dopamine at poly (solochrome cyanine)/Pd nanoparticles doped modified carbon paste electrode and simultaneous resolution in the presence of ascorbic acid and uric acid: A voltammetric method, *Anal*. *Methods*, **5** (2013): 5627–5636. https://doi.org/10.1039/c3ay41039k.